

Electroassociation of Ultracold Dipolar Molecules into Tetramer Field-Linked States

Goulven Quéméner[✉]*Université Paris-Saclay, CNRS, Laboratoire Aimé Cotton, 91405 Orsay, France*John L. Bohn[✉]*JILA, NIST, and Department of Physics, University of Colorado, Boulder, Colorado 80309-0440, USA*James F. E. Croft[✉]*The Dodd-Walls Centre for Photonic and Quantum Technologies, Dunedin 9054, New Zealand
and Department of Physics, University of Otago, Dunedin 9054, New Zealand* (Received 19 April 2023; revised 19 June 2023; accepted 22 June 2023; published 26 July 2023)

The presence of electric or microwave fields can modify the long-range forces between ultracold dipolar molecules in such a way as to engineer weakly bound states of molecule pairs. These so-called field-linked states [A. V. Avdeenkov and J. L. Bohn, *Phys. Rev. Lett.* **90**, 043006 (2003).; L. Lassablière and G. Quéméner, *Phys. Rev. Lett.* **121**, 163402 (2018).], in which the separation between the two bound molecules can be orders of magnitude larger than the molecules themselves, have been observed as resonances in scattering experiments [X.-Y. Chen *et al.*, *Nature (London)* **614**, 59 (2023).]. Here, we propose to use them as tools for the assembly of weakly bound tetramer molecules, by means of ramping an electric field, the electric-field analog of magnetoassociation in atoms. This ability would present new possibilities for constructing ultracold polyatomic molecules.

DOI: [10.1103/PhysRevLett.131.043402](https://doi.org/10.1103/PhysRevLett.131.043402)

Field-linked states (FLS) appear in carefully engineered long-range wells, of two colliding ultracold molecules. The wells are created by applying an external field when the molecules are in a specific initial state. They were first predicted in 2003 [1–4] using a static electric field. In 2018 [5], a second type of FLS was predicted using a blue-detuned microwave field on ground-state ultracold dipolar molecules. In 2023, resonances due to this second type of “microwave” FLS were experimentally observed [6]. This discovery opens a wide range of possibilities that have so far been lacking for ultracold molecules, the most important being the ability to control the molecule-molecule scattering length at will [5], from positive to negative, from a small to a large value. This control is key in order to reach the regime needed to explore strongly correlated states of matter involving molecular Bose-Einstein condensates (BECs) and degenerate Fermi gases (DFGs) [7–9], made possible by the electric dipole moment of the molecules. For example, studying the BEC-BCS crossover [10–13] could now be within reach for fermionic dipolar molecules, in a regime where few-body dipolar physics could come into play [14]. Similarly, studies of Efimov physics [15–17] with bosonic dipolar molecules [18] could also be made possible. Finally, one could tune both the scattering length and the dipolar length in an electric dipolar molecular BEC to explore density profiles with supersolid properties [19], complementing those already observed for magnetic dipolar atomic BECs [20–22].

The ability to use a magnetic field to control the scattering length via Fano-Feshbach resonances, as can be done between atoms [23,24] or between atoms and molecules [25,26], seems to rarely occur between alkali molecules. Except for the lightest alkali molecule of LiNa in the triplet electronic state [27], it has proven somewhat difficult to find well-isolated resonances in heavy molecule-molecule systems in their ground electronic singlet states, due to their high density of states (see, for example, [28–30]). The existence of FLS could circumvent this difficulty and present an alternative way to both shield the molecules against losses and tune the scattering length.

In addition, we note the power of magnetic field ramps to produce bound atomic dimers across Fano-Feshbach resonances [23,24]. Here, we explore the feasibility of associating two ultracold dipolar molecules into a long-range, field-linked tetramer state, using an electric field. Such a technique promises to be a powerful starting point for the controlled assembly of polyatomic molecules, starting from diatomic ingredients. By ramping the electric field of a microwave, we show that electroassociation (EA) of two colliding dipolar molecules can be achieved using experimentally realistic ramps and traps. We discuss the conditions under which EA is applicable, particularly in terms of the initial population distribution of the molecular gas and the bosonic or fermionic character of the molecules.

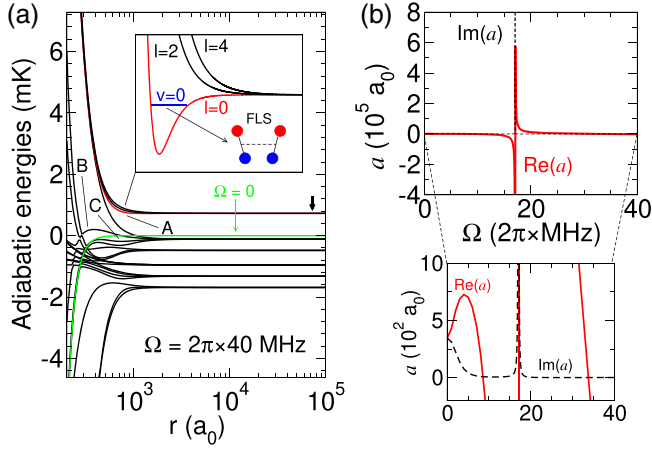


FIG. 1. (a) Potentials of two colliding molecules as a function of the intermolecular separation r , for $\Delta = 2\pi \times 10$ MHz and $\Omega = 2\pi \times 40$ MHz. The initial colliding state is indicated by an arrow. The red curve shows the $l = 0$ entrance channel. The green curve shows the analogous channel in the absence of microwave shielding ($\Omega = 0$). The inset shows an enlargement of the long-range well in red that can carry a FLS. The letters A, B, and C label, respectively, the entrance channel and two scattering channels into which the FLS can decay. (b) Scattering length a as a function of Ω for $\Delta = 2\pi \times 10$ MHz.

We first consider an ultracold gas of dipolar bosonic bialkali molecules in their ground electronic, vibrational, and rotational state, taking $^{23}\text{Na}^{87}\text{Rb}$ as a representative example [31,32]. Many other molecules have been created under similar conditions [33–42] and can also be considered without loss of generality. When a circularly polarized microwave field is applied on molecules in their ground rotational state $j = 0$, and if the microwave is slightly blue detuned with respect to the first excited state $j = 1$ with an energy detuning $\hbar\Delta$, it was proposed [5,43] and observed [9,44–46] that a shielding against collisional losses takes place at appropriate values of the Rabi frequency $\Omega = dE/\hbar$, enabling long-lived molecules. Ω is proportional to the electric field E of the microwave and the electric dipole moment d of the molecule.

Potentials that lead to shielding of two colliding NaRb molecules are shown in Fig. 1(a), where they are plotted as a function of the intermolecular separation r , for $\Delta = 2\pi \times 10$ MHz and $\Omega = 2\pi \times 40$ MHz. The initial colliding state (entrance channel) is indicated by a black arrow, corresponding to two molecules in $j = 0$. In this situation, the potentials of the entrance channel become repulsive at $r \approx 10^3 a_0$ when dressed by the microwave. Also, transitions between the initial collisional state and the lower ones become weak. This prevents most of the molecules from being lost due to any short-range loss mechanism or from being excited in $j = 1$ [5,43]. The red curve corresponds to the entrance channel for the $l = 0$ partial wave. To compare, the analogous curve is shown in the absence of microwave ($\Omega = 0$) as a green dashed line, and, as it is

attractive in that case, it cannot shield the molecules against losses. The red curve is also shown in the inset in the figure (we emphasize that the radial coordinate axis in Fig. 1 is on a logarithmic scale highlighting the extremely long-range nature of these states). The two other black curves of the inset correspond to an entrance channel with $l = 2$ and $l = 4$. The values of l are even, as we are considering indistinguishable bosonic molecules. The $l = 0$ curve is attractive at long range as expected for an s wave, before getting repulsive from the shielding. This creates a long-range well that can hold a FLS [1–4], represented in blue and characterized by a quantum number $v = 0$. The $l = 2$ and $l = 4$ curves are already repulsive at long range due to the presence of the associated centrifugal barriers and do not form wells. As such, in the following we will solely focus on the s -wave curve, in which the FLS exists. Presumably, similar conclusions on the control of the scattering length and the existence of FLS also apply to optical shielding [47–49], providing an alternative route for experimental investigations.

The presence of a FLS enables the tunability of the scattering length, as can be seen in Fig. 1(b). Generally, the scattering length a is a complex quantity [50,51] expressed as $a = \text{Re}(a) - i\text{Im}(a)$ with $\text{Im}(a) \geq 0$. This quantity can be linked to the two-body elastic and quenching rate coefficients [52]. When Ω is varied from 0 to $2\pi \times 40$ MHz, $\text{Re}(a)$ diverges and changes sign at $\Omega \approx 2\pi \times 17$ MHz, from a big negative value to a big positive value. This is related to the appearance at threshold of a new bound state in the long-range well and is the origin of the FLS seen at $2\pi \times 40$ MHz in Fig. 1(a). Such a variation of the scattering length is reminiscent of magnetoassociation (MA), where now the electric field (via Ω) plays the role of the magnetic field. As such, one can use a similar technique to associate two molecules, hence the name “electroassociation.”

We now consider the effect of a trapping potential on the molecular collisions, which causes the relative motion between molecules to be quantized [60,61]. In the experiments cited above, the molecules are generally trapped in an optical dipole trap (ODT), that can be well represented by a harmonic potential. To simplify the study, we will consider a spherical ODT with a unique frequency $\nu = 100$ Hz. The trapping potential is then given by $U_{\text{trap}}(r_i) = m\omega^2 r_i^2/2$, with $\omega = 2\pi\nu$, m the mass of a molecule, and r_i the position of molecule i , with $i = 1, 2$. To treat the collision between two molecules, we use coordinates for the relative motion in the center-of-mass frame [60–62], as the center of mass is not involved in the process. One can then show that, for identical molecules seeing the same frequency ν of the trap, the problem can be recast using a trapping potential for the relative motion given by $U_{\text{trap}}(r) = \mu\omega^2 r^2/2$, where $\mu = m/2$ is the reduced mass of the two molecules and r the intermolecular separation. As the center-of-mass motion is independent and uncoupled from the relative motion, it is not taken into account in the following.

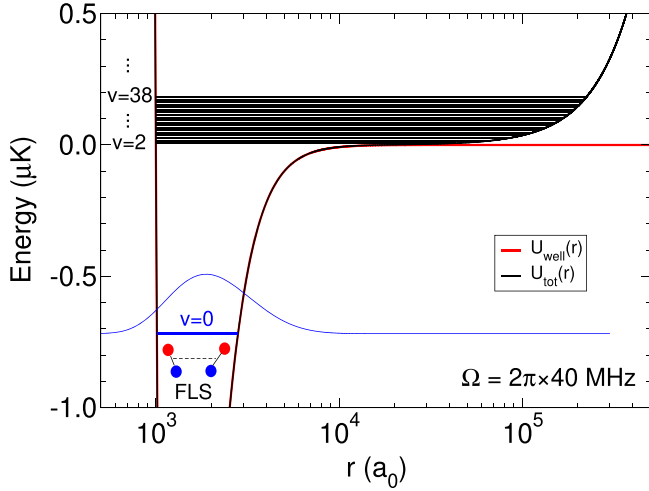


FIG. 2. Energies E_v of the eigenstates (blue and black horizontal lines) in the potential energy U_{tot} (black curve) comprised of the long-range well U_{well} in Fig. 1(a) (red curve) and the trapping potential of the molecules U_{trap} , for $\nu = 100$ Hz and $l = 0$. The FLS is plotted in blue with $v = 0$ and negative energy; the HOS are plotted in black with $v = 2, \dots, 38$ and positive energies. This is an example for $\Delta = 2\pi \times 10$ MHz and $\Omega = 2\pi \times 40$ MHz.

The overall potential $U_{\text{tot}}(r)$ seen by two ultracold molecules in $j = 0$ is then composed of the long-range well $U_{\text{well}}(r)$, shown in red in Fig. 1(a) and the trapping potential $U_{\text{trap}}(r)$. This potential is plotted in Fig. 2 and shows its spatial extent. The discrete energies of the molecules are shown in blue for the lowest state along with the corresponding wave function and in black for the higher states. The energies were computed numerically by solving the radial Schrödinger equation for a given value of Ω , for the Hamiltonian $H(r) = -(\hbar^2/2\mu)d^2/dr^2 + U_{\text{tot}}(r)$ for $l = 0$. Each energy and wave function is characterized by a quantum number $k = 0, 1, 2, \dots$ that counts the number of the state. The energies E_k and wave functions $f_k(r)$ are found when the outward and inward log derivative of the wave functions match [63–65]. For low values of Ω when the long-range well is not too deep, the energies tend to those of the spherical harmonic oscillator given by $E_v^{\text{ho}} = \hbar\omega(v + 3/2)$, with $v = 2k + l$ [60,61]. A state v has a degeneracy $g_v = (v + 1)(v + 2)/2$. l is the quantum number associated with the orbital angular momentum of the relative motion in the spherical harmonic potential and is the same value as the partial wave introduced above when two particles collide. For indistinguishable bosonic molecules, v takes even values, as l are even. If we would have considered indistinguishable fermionic molecules, v would have taken odd values, as l would have been odd. In our study, we consider just $l = 0$, as higher values $l = 2, 4, \dots$ are not relevant, as they do not provide conditions for the existence of FLS. Then, $v \equiv 2k$ and $v = 0, 2, \dots$. For fermions, we would have had $v = 1, 3, \dots$. Typically, at $\nu = 100$ Hz, $E_0^{\text{ho}} \simeq 7.2$ nK, $E_2^{\text{ho}} \simeq 16.8$ nK, etc. We will

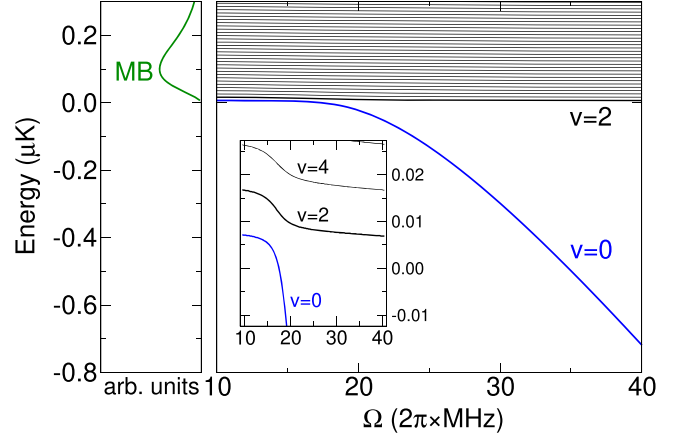


FIG. 3. Energies E_v of many eigenstates shown in Fig. 2 for $l = 0$, now as a function of Ω . The inset shows an enlargement of the avoided crossing between the state $v = 0$ and $v = 2$. The left panel shows a typical initial Maxwell-Boltzmann distribution of an individual molecule for $T = 50$ nK.

refer to an eigenstate of positive energy as an harmonic oscillator state (HOS) and to an eigenstate of negative energy as a FLS. For each value of Ω at $\Delta = 2\pi \times 10$ MHz, we compute the energy E_v of the eigenstates. This is shown in Fig. 3. The lowest state $v = 0$ is plotted in blue. At low values of Ω , $E_0 \simeq E_0^{\text{ho}}$, no FLS exists, the energy being simply the one of the lowest HOS. When Ω increases, the energy E_0 decreases and becomes negative around the value $\Omega = 2\pi \times 17$ MHz. Then the lowest HOS transfers smoothly to the FLS. Not surprisingly, this occurs at the same value of Ω where the scattering length diverges, as seen in Fig. 1.

These results are very reminiscent of trapping potentials for MA [60,61], even though the physical principle behind the curves is very different. Most notably, only one potential energy curve is sufficient for EA, while two are needed for MA. The idea behind electroassociation is to pass smoothly from the lowest HOS, initially populated by the free well-separated molecules, to the bound tetramer FLS, by ramping the value of Ω as a function of time via the electric field of the microwave. Solving the time-dependent Schrödinger equation including the contribution of the decay lifetimes of the diatomic molecules or the tetramers yields the time evolution of the probability $P_{vv'}$ [52] to start in a state v and end up in a state v' for the $l = 0$ curve, for a given ramp noted $R = d\Omega/dt$ with R expressed here in $2\pi \times \text{MHz/ms}$.

For illustrative purposes, we consider a ramp from $\Omega = 2\pi \times 10$ MHz to $\Omega = 2\pi \times 40$ MHz. The probability P_{00} to start in $v = 0$ and end up in $v' = 0$ is shown as a black solid line in Fig. 4, as a function of the value of the ramp R , for $\nu = 100$ Hz. We can see that the probability reaches a maximum for a ramp of $R \simeq 2\pi \times 3.4$ MHz/ms, corresponding to a duration of 8.8 ms for which an association probability of 75% can be reached. This shows that one can

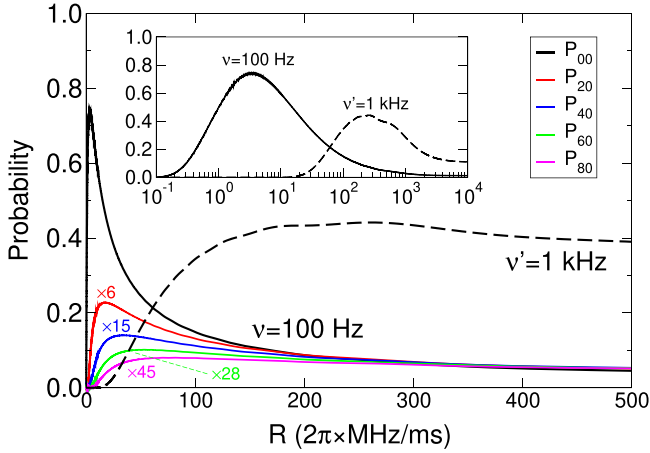


FIG. 4. Probability P_{00} to start in the state $v = 0$ (representing two trapped molecules) at $\Omega = 2\pi \times 10$ MHz and finish in the state $v' = 0$ (representing a FLS) at $\Omega = 2\pi \times 40$ MHz, for trap frequencies of $\nu = 100$ Hz (black solid line) and $\nu' = 1$ kHz (black dashed line). This is plotted as a function of the applied ramp R . The inset shows the same figure using a logarithmic scale. The lower curves show the probabilities P_{v0} at $\Omega = 2\pi \times 40$ MHz for $\nu = 100$ Hz, with $v = 2, 4, 6, 8$ shown as red, blue, green, and pink lines, respectively. For visibility in the figure, we have multiplied them by 6, 15, 28, and 45, respectively.

have relatively efficient EA of two molecules initially in the lowest HOS of the relative motion $v = 0$ into a long-range tetramer under realistic experimental conditions. The range of application is, however, limited (see the inset). One needs to remain in the range $R = 2\pi \times [1-10]$ MHz/ms, to get probabilities above 50%. The optimal ramp is a balance between two competing mechanisms. If the ramp is too slow ($R < 2\pi \times 1$ MHz/ms), then collisions lead to molecule loss during the ramp, and the final yield of FLS will be small. On the other hand, if the ramp is too fast ($R > 2\pi \times 10$ MHz/ms), the molecules are unable to adiabatically transfer into the ground state $v' = 0$, with the result that higher trap states are populated rather than the FLS.

In Fig. 4, we also show the probabilities P_{v0} to start in the $l = 0$ curve of a state $v = 2, 4, 6, 8$ of the HOS and to end up in $v' = 0$, that is, the FLS. We see that P_{00} is clearly always higher than the other probabilities P_{v0} with $v > 0$, whatever the choice of ramp, the other probabilities being less than 4%. Besides the criterion of appropriate ramps, this shows that EA is also most efficient when the relative motion of bosonic molecules occupy the lowest HOS $v = 0$. The same conclusion will also hold for fermionic molecules except that the lowest HOS would be $v = 1$. In the higher states, the probabilities become very small and no real chance is given to form a FLS.

As such, the initial distribution will strongly affect the efficiency of the formation of a FLS. First, we take the example of a initial Maxwell-Boltzmann distribution for indistinguishable bosonic molecules, for which the

population of a state v_i for an individual molecule $i = 1, 2$ is given by $Ag_{v_i} \exp(-E_{v_i}^{\text{ho}}/k_B T)$, where A is the normalization factor and g_{v_i} the degeneracy of state v_i . We show an example distribution in the left panel in Fig. 3 as a function of the discrete energy of an individual trapped molecule for a typical temperature of $T = 50$ nK. The distribution shows that the molecules populate dominantly high excited states, namely, $v_1, v_2 \simeq 20$ at that temperature. To express the distribution of two individual molecules $i = 1, 2$ in the relative and center-of-mass representation in which the previously derived results hold, we have to use the composition of the harmonic oscillator functions derived, for example, in Appendix C in Ref. [62]. It is shown that, for any symmetric constructions in the individual representation between the v_1 and v_2 states, there will be always a $v = 0$ component in the relative one. For a thermal gas of indistinguishable fermionic molecules, it is also shown in Appendix C in Ref. [62] that, for any antisymmetric construction of v_1 and v_2 states, there will be always a corresponding $v = 1$ component with the difference with the bosonic case now that one has to have $v_1 \neq v_2$ (by definition of antisymmetric states). Then, any vibrational state populated at a given temperature T in Fig. 3 will have at least some projection onto a $v = 0$ state for bosons (or a $v = 1$ state for fermions) and can contribute to EA. This statement is in agreement with former results obtained in the context of MA of ultracold bosonic and fermionic atoms into weakly bound molecules [66].

We finally consider starting from a BEC. In this case, all the molecules start in the lowest state $v_1 = v_2 = 0$ which is equivalent to occupying the $v = 0$ state. To illustrate the feasibility of such an example, one has to take into account the many-body interactions in a BEC [60,61,67,68]. Here we follow the work of Ref. [67], where the authors showed that one can rescale the trap frequency to a new effective one, $\nu' = (\hbar/2m)(n/2)^{2/3}$. For example, a typical BEC density of $n = 1.3 \times 10^{13}$ molecules/cm³ yields an effective confinement of $\nu' = 1$ kHz for NaRb. As shown in Fig. 4, the probability P_{00} at such frequency now reaches a maximum for a ramp of $R \simeq 2\pi \times 260$ MHz/ms, corresponding to a duration of 0.11 ms. The optimal association probability is only 44%, which is lower than for $\nu = 100$ Hz. This is because in a BEC the density is much higher and collisions are, therefore, more frequent, decreasing the overall efficiency of EA. As such, the optimal ramp has to be faster compared to the $\nu = 100$ Hz case. This can be afforded in this case, as the rescaled trap frequency ν' is higher than ν . The avoided crossing seen in Fig. 3 will now be more avoided, still allowing a high transfer to the FLSs even at such a large ramp. In the situation of a molecular DFG [7–9], one could also consider starting with distinguishable fermions as was done in the context of MA, provided that the microwave shielding and the existence of FLS still hold for that case. If that is the case, $l = 0$ and

$v = 0$ would be allowed, as well as symmetric constructions of v_1 and v_2 states, increasing the number of combinations of v_1 and v_2 allowed and the conversion rate for the fermionic case.

In conclusion, we have shown that electroassociation of two ultracold dipolar molecules into a tetramer field-linked state is possible using realistic ramps of the electric field of a microwave, when the molecules are in the ground state of their relative motion. For typical thermal gases with typical densities and typical harmonic traps used in experiments, any vibrational state of a Maxwell-Boltzmann distribution can contribute to EA. An ideal situation occurs for typical BEC conditions, where most of the molecules are directly in the ground state of their relative motion. But, in both cases, EA efficiency is affected by collisional losses. To further prevent such collisions, one could consider starting with exactly two molecules in the ground state of a strong confined trap such as an optical lattice [7,32,69–71] or optical tweezers [39,40,44,72–75]. This could be an ideal setup for future prospects of transferring such long-range bound excited states to ground-state tetramers, as was done in the context of formation of diatomic molecules using stimulated Raman adiabatic processes [76–78]. This constitutes an alternative to photoassociation proposals [53,79–83] and could open the way for a piece-by-piece production of ultracold polyatomic molecules.

J. L. B. acknowledges that this material is based upon work supported by the National Science Foundation under Grant No. PHY 1734006. J. F. E. C. acknowledges the support of the Marsden Fund Council from Government funding, managed by Royal Society Te Apārangi (Project ID 19-UOO-130), as well as a Dodd-Wall Fellowship.

Note added.—Recently, we became aware that electro-association of two fermionic molecules into a tetramer field-linked state has been experimentally realized and observed [84].

[1] A. V. Avdeenkov and J. L. Bohn, *Phys. Rev. Lett.* **90**, 043006 (2003).
 [2] A. V. Avdeenkov and J. L. Bohn, *Phys. Rev. A* **66**, 052718 (2002).
 [3] A. V. Avdeenkov, D. C. E. Bortolotti, and J. L. Bohn, *Phys. Rev. A* **69**, 012710 (2004).
 [4] A. V. Avdeenkov and J. L. Bohn, *Phys. Rev. A* **71**, 022706 (2005).
 [5] L. Lassablière and G. Quéméner, *Phys. Rev. Lett.* **121**, 163402 (2018).
 [6] X.-Y. Chen, A. Schindewolf, S. Eppelt, R. Bause, M. Duda, S. Biswas, T. Karman, T. Hilker, I. Bloch, and X.-Y. Luo, *Nature (London)* **614**, 59 (2023).
 [7] L. De Marco, G. Valtolina, K. Matsuda, W. G. Tobias, J. P. Covey, and J. Ye, *Science* **363**, 853 (2019).

[8] G. Valtolina, K. Matsuda, W. G. Tobias, J.-R. Li, L. De Marco, and J. Ye, *Nature (London)* **588**, 239 (2020).
 [9] A. Schindewolf, R. Bause, X.-Y. Chen, M. Duda, T. Karman, I. Bloch, and X.-Y. Luo, *Nature (London)* **607**, 677 (2022).
 [10] C. A. Regal, M. Greiner, and D. S. Jin, *Phys. Rev. Lett.* **92**, 040403 (2004).
 [11] M. Bartenstein, A. Altmeyer, S. Riedl, S. Jochim, C. Chin, J. H. Denschlag, and R. Grimm, *Phys. Rev. Lett.* **92**, 120401 (2004).
 [12] M. W. Zwierlein, C. A. Stan, C. H. Schunck, S. M. F. Raupach, A. J. Kerman, and W. Ketterle, *Phys. Rev. Lett.* **92**, 120403 (2004).
 [13] T. Bourdel, L. Khaykovich, J. Cubizolles, J. Zhang, F. Chevy, M. Teichmann, L. Tarruell, S. J. J. M. F. Kokkelmans, and C. Salomon, *Phys. Rev. Lett.* **93**, 050401 (2004).
 [14] Y. Wang, J. P. D’Incao, and C. H. Greene, *Phys. Rev. Lett.* **107**, 233201 (2011).
 [15] V. Efimov, *Phys. Lett. B* **33**, 563 (1970).
 [16] T. Kraemer, M. Mark, P. Waldburger, J. G. Danzl, C. Chin, B. Engeser, A. D. Lange, K. Pilch, A. Jaakkola, H.-C. Nägerl *et al.*, *Nature (London)* **440**, 315 (2006).
 [17] E. Braaten and H.-W. Hammer, *Phys. Rep.* **428**, 259 (2006).
 [18] Y. Wang, J. P. D’Incao, and C. H. Greene, *Phys. Rev. Lett.* **106**, 233201 (2011).
 [19] M. Schmidt, L. Lassablière, G. Quéméner, and T. Langen, *Phys. Rev. Res.* **4**, 013235 (2022).
 [20] L. Tanzi, E. Lucioni, F. Famà, J. Catani, A. Fioretti, C. Gabbanini, R. N. Bisset, L. Santos, and G. Modugno, *Phys. Rev. Lett.* **122**, 130405 (2019).
 [21] L. Chomaz, D. Petter, P. Ilzhöfer, G. Natale, A. Trautmann, C. Politi, G. Durastante, R. M. W. van Bijnen, A. Patscheider, M. Sohmen *et al.*, *Phys. Rev. X* **9**, 021012 (2019).
 [22] F. Böttcher, J.-N. Schmidt, M. Wenzel, J. Hertkorn, M. Guo, T. Langen, and T. Pfau, *Phys. Rev. X* **9**, 011051 (2019).
 [23] T. Köhler, K. Góral, and P. S. Julienne, *Rev. Mod. Phys.* **78**, 1311 (2006).
 [24] C. Chin, R. Grimm, P. Julienne, and E. Tiesinga, *Rev. Mod. Phys.* **82**, 1225 (2010).
 [25] H. Yang, D.-C. Zhang, L. Liu, Y.-X. Liu, J. Nan, B. Zhao, and J.-W. Pan, *Science* **363**, 261 (2019).
 [26] H. Yang, X.-Y. Wang, Z. Su, J. Cao, D.-C. Zhang, J. Rui, B. Zhao, C.-L. Bai, and J.-W. Pan, *Nature (London)* **602**, 229 (2022).
 [27] J. J. Park, Y.-K. Lu, A. O. Jamison, T. V. Tscherbul, and W. Ketterle, *Nature (London)* **614**, 54 (2023).
 [28] J. F. E. Croft, J. L. Bohn, and G. Quéméner, *Phys. Rev. A* **102**, 033306 (2020).
 [29] J. F. E. Croft, J. L. Bohn, and G. Quéméner, *Phys. Rev. A* **107**, 023304 (2023).
 [30] R. Bause, A. Christianen, A. Schindewolf, I. Bloch, and X.-Y. Luo, *J. Phys. Chem. A* **127**, 729 (2023).
 [31] M. Guo, B. Zhu, B. Lu, X. Ye, F. Wang, R. Vexiau, N. Bouloufa-Maafa, G. Quéméner, O. Dulieu, and D. Wang, *Phys. Rev. Lett.* **116**, 205303 (2016).
 [32] L. Christakis, J. S. Rosenberg, R. Raj, S. Chi, A. Morningstar, D. A. Huse, Z. Z. Yan, and W. S. Bakr, *Nature (London)* **614**, 64 (2023).

- [33] K.-K. Ni, S. Ospelkaus, M. H. G. de Miranda, A. Pe'er, B. Neyenhuis, J. J. Zirbel, S. Kotochigova, P. S. Julienne, D. S. Jin, and J. Ye, *Science* **322**, 231 (2008).
- [34] K. Aikawa, D. Akamatsu, M. Hayashi, K. Oasa, J. Kobayashi, P. Naidon, T. Kishimoto, M. Ueda, and S. Inouye, *Phys. Rev. Lett.* **105**, 203001 (2010).
- [35] T. Takekoshi, L. Reichsöllner, A. Schindewolf, J. M. Hutson, C. R. Le Sueur, O. Dulieu, F. Ferlaino, R. Grimm, and H.-C. Nägerl, *Phys. Rev. Lett.* **113**, 205301 (2014).
- [36] P. K. Molony, P. D. Gregory, Z. Ji, B. Lu, M. P. Köppinger, C. R. Le Sueur, C. L. Blackley, J. M. Hutson, and S. L. Cornish, *Phys. Rev. Lett.* **113**, 255301 (2014).
- [37] J. W. Park, S. A. Will, and M. W. Zwierlein, *Phys. Rev. Lett.* **114**, 205302 (2015).
- [38] T. M. Rvachov, H. Son, A. T. Sommer, S. Ebadi, J. J. Park, M. W. Zwierlein, W. Ketterle, and A. O. Jamison, *Phys. Rev. Lett.* **119**, 143001 (2017).
- [39] L. R. Liu, J. D. Hood, Y. Yu, J. T. Zhang, N. R. Hutzler, T. Rosenband, and K.-K. Ni, *Science* **360**, 900 (2018).
- [40] L. Anderegg, L. W. Cheuk, Y. Bao, S. Burchesky, W. Ketterle, K.-K. Ni, and J. M. Doyle, *Science* **365**, 1156 (2019).
- [41] K. K. Voges, P. Gersema, M. Meyer zum Alten Borgloh, T. A. Schulze, T. Hartmann, A. Zenesini, and S. Ospelkaus, *Phys. Rev. Lett.* **125**, 083401 (2020).
- [42] I. Stevenson, A. Z. Lam, N. Bigagli, C. Warner, W. Yuan, S. Zhang, and S. Will, *Phys. Rev. Lett.* **130**, 113002 (2023).
- [43] T. Karman and J. M. Hutson, *Phys. Rev. Lett.* **121**, 163401 (2018).
- [44] L. Anderegg, S. Burchesky, Y. Bao, S. S. Yu, T. Karman, E. Chae, K.-K. Ni, W. Ketterle, and J. M. Doyle, *Science* **373**, 779 (2021).
- [45] N. Bigagli, C. Warner, W. Yuan, S. Zhang, I. Stevenson, T. Karman, and S. Will, [arXiv:2303.16845](https://arxiv.org/abs/2303.16845).
- [46] J. Lin, G. Chen, M. Jin, Z. Shi, F. Deng, W. Zhang, G. Quéméner, T. Shi, S. Yi, and D. Wang, [arXiv:2304.08312](https://arxiv.org/abs/2304.08312).
- [47] T. Xie, M. Lepers, R. Vexiau, A. Orbán, O. Dulieu, and N. Bouloufa-Maafa, *Phys. Rev. Lett.* **125**, 153202 (2020).
- [48] C. Karam, M. Meyer zum Alten Borgloh, R. Vexiau, M. Lepers, S. Ospelkaus, N. Bouloufa-Maafa, L. Karpa, and O. Dulieu, [arXiv:2211.08950](https://arxiv.org/abs/2211.08950).
- [49] R. Napolitano, J. Weiner, and P. S. Julienne, *Phys. Rev. A* **55**, 1191 (1997).
- [50] N. Balakrishnan, V. Kharchenko, R. Forrey, and A. Dalgarno, *Chem. Phys. Lett.* **280**, 5 (1997).
- [51] J. M. Hutson, *New J. Phys.* **9**, 152 (2007).
- [52] See Supplemental Material at <http://link.aps.org/supplemental/10.1103/PhysRevLett.131.043402> for the description of the relations between the scattering matrix and the observables, the time-dependent dynamics during the ramp, and the dissociation lifetime of the FLS, which includes Refs. [3,5,28–30,51,53–59].
- [53] M. Lepers, R. Vexiau, M. Aymar, N. Bouloufa-Maafa, and O. Dulieu, *Phys. Rev. A* **88**, 032709 (2013).
- [54] M. L. González-Martínez, J. L. Bohn, and G. Quéméner, *Phys. Rev. A* **96**, 032718 (2017).
- [55] H. A. Bethe, *Phys. Rev.* **47**, 747 (1935).
- [56] E. P. Wigner, *Phys. Rev.* **73**, 1002 (1948).
- [57] Z. Idziaszek and P. S. Julienne, *Phys. Rev. Lett.* **104**, 113202 (2010).
- [58] H. Friedrich, *Theoretical Atomic Physics* (Springer, New York, 2005).
- [59] B. H. Brandsen and C. J. Joachain, *Physics of Atoms and Molecules* (Addison-Wesley, New York, 2003).
- [60] F. H. Mies, E. Tiesinga, and P. S. Julienne, *Phys. Rev. A* **61**, 022721 (2000).
- [61] E. Tiesinga, C. J. Williams, F. H. Mies, and P. S. Julienne, *Phys. Rev. A* **61**, 063416 (2000).
- [62] G. Quéméner and J. L. Bohn, *Phys. Rev. A* **83**, 012705 (2011).
- [63] B. R. Johnson, *J. Chem. Phys.* **67**, 4086 (1977).
- [64] J. M. Hutson, *Comput. Phys. Commun.* **84**, 1 (1994).
- [65] A. E. Thornley and J. M. Hutson, *J. Chem. Phys.* **101**, 5578 (1994).
- [66] E. Hodby, S. T. Thompson, C. A. Regal, M. Greiner, A. C. Wilson, D. S. Jin, E. A. Cornell, and C. E. Wieman, *Phys. Rev. Lett.* **94**, 120402 (2005).
- [67] B. Borca, D. Blume, and C. H. Greene, *New J. Phys.* **5**, 111 (2003).
- [68] K. Góral, T. Köhler, S. A. Gardiner, E. Tiesinga, and P. S. Julienne, *J. Phys. B* **37**, 3457 (2004).
- [69] M. H. G. de Miranda, A. Chotia, B. Neyenhuis, D. Wang, G. Quéméner, S. Ospelkaus, J. Bohn, J. L. Ye, and D. S. Jin, *Nat. Phys.* **7**, 502 (2011).
- [70] A. Chotia, B. Neyenhuis, S. A. Moses, B. Yan, J. P. Covey, M. Foss-Feig, A. M. Rey, D. S. Jin, and J. Ye, *Phys. Rev. Lett.* **108**, 080405 (2012).
- [71] B. Yan, S. A. Moses, B. Gadway, J. P. Covey, K. R. A. Hazzard, A. M. Rey, D. S. Jin, and J. Ye, *Nature (London)* **501**, 521 (2013).
- [72] A. M. Kaufman and K.-K. Ni, *Nat. Phys.* **17**, 1324 (2021).
- [73] D. K. Ruttley, A. Guttridge, S. Spence, R. C. Bird, C. R. Le Sueur, J. M. Hutson, and S. L. Cornish, *Phys. Rev. Lett.* **130**, 223401 (2023).
- [74] C. M. Holland, Y. Lu, and L. W. Cheuk, [arXiv:2210.06309](https://arxiv.org/abs/2210.06309).
- [75] Y. Bao, S. S. Yu, L. Anderegg, E. Chae, W. Ketterle, K.-K. Ni, and J. M. Doyle, [arXiv:2211.09780](https://arxiv.org/abs/2211.09780).
- [76] K. Bergmann, H. Theuer, and B. W. Shore, *Rev. Mod. Phys.* **70**, 1003 (1998).
- [77] K. Bergmann, N. V. Vitanov, and B. W. Shore, *J. Chem. Phys.* **142**, 170901 (2015).
- [78] N. V. Vitanov, A. A. Rangelov, B. W. Shore, and K. Bergmann, *Rev. Mod. Phys.* **89**, 015006 (2017).
- [79] J. Pérez-Ríos, M. Lepers, and O. Dulieu, *Phys. Rev. Lett.* **115**, 073201 (2015).
- [80] J. Schnabel, T. Kampschulte, S. Rupp, J. Hecker Denschlag, and A. Köhn, *Phys. Rev. A* **103**, 022820 (2021).
- [81] M. Gacesa, J. N. Byrd, J. Smucker, J. A. Montgomery, and R. Côté, *Phys. Rev. Res.* **3**, 023163 (2021).
- [82] A. A. Elkamshishy and C. H. Greene, *J. Phys. Chem. A* **127**, 18 (2023).
- [83] B. Shammout, L. Karpa, S. Ospelkaus, E. Tiemann, and O. Dulieu, [arXiv:2303.11891](https://arxiv.org/abs/2303.11891).
- [84] X.-Y. Chen, S. Biswas, S. Eppelt, A. Schindewolf, F. Deng, T. Shi, S. Yi, T. A. Hilker, I. Bloch, and X.-Y. Luo, [arXiv:2306.00962](https://arxiv.org/abs/2306.00962).